

## Few- and many-nucleon systems with semilocal coordinate-space regularized chiral two- and three-body forces

E. Epelbaum,<sup>1</sup> J. Golak,<sup>2</sup> K. Hebeler,<sup>3</sup> T. Hüther,<sup>3</sup> H. Kamada,<sup>4</sup> H. Krebs,<sup>1</sup> P. Maris,<sup>5</sup> Ulf-G. Meißner,<sup>6,7,8</sup> A. Nogga,<sup>7</sup>  
R. Roth,<sup>3</sup> R. Skibiński,<sup>2</sup> K. Topolnicki,<sup>2</sup> J. P. Vary,<sup>5</sup> K. Vobig,<sup>3</sup> and H. Witała<sup>2</sup>  
(LENPIC Collaboration)

<sup>1</sup>*Ruhr-Universität Bochum, Fakultät für Physik und Astronomie, Institut für Theoretische Physik II, D-44780 Bochum, Germany*

<sup>2</sup>*M. Smoluchowski Institute of Physics, Jagiellonian University, PL-30348 Kraków, Poland*

<sup>3</sup>*Institut für Kernphysik, Technische Universität Darmstadt, 64289 Darmstadt, Germany*

<sup>4</sup>*Department of Physics, Faculty of Engineering, Kyushu Institute of Technology, Kitakyushu 804-8550, Japan*

<sup>5</sup>*Department of Physics and Astronomy, Iowa State University, Ames, Iowa 50011, USA*

<sup>6</sup>*Helmholtz-Institut für Strahlen- und Kernphysik and Bethe Center for Theoretical Physics, Universität Bonn, D-53115 Bonn, Germany*

<sup>7</sup>*Institut für Kernphysik, Institute for Advanced Simulation and Jülich Center for Hadron Physics,  
Forschungszentrum Jülich, D-52425 Jülich, Germany*

<sup>8</sup>*JARA - High Performance Computing, Forschungszentrum Jülich, D-52425 Jülich, Germany*



(Received 26 July 2018; revised manuscript received 5 January 2019; published 19 February 2019)

We present calculations of nucleon-deuteron scattering as well as ground and low-lying excited states of light nuclei in the mass range  $A = 3\text{--}16$  up through next-to-next-to-leading order in chiral effective field theory using semilocal coordinate-space regularized two- and three-nucleon forces. It is shown that both of the low-energy constants entering the three-nucleon force at this order can be determined from the triton binding energy and the differential cross section minimum in elastic nucleon-deuteron scattering. From all considered nucleon-deuteron scattering observables, the strongest constraint on these low-energy constants emerges from the precisely measured cross section minimum at  $E_N = 70$  MeV. The inclusion of the three-nucleon force is found to improve the agreement with the data for most of the considered observables.

DOI: [10.1103/PhysRevC.99.024313](https://doi.org/10.1103/PhysRevC.99.024313)

### I. INTRODUCTION

Chiral effective field theory (EFT) offers a convenient and powerful framework to analyze low-energy properties of few- and many-body nuclear systems in harmony with the symmetries (and their breaking pattern) of QCD (see Refs. [1–3] for review articles). In recent years, the chiral expansion of the two-nucleon ( $NN$ ) force, the dominant part of the nuclear Hamiltonian, has been pushed to fifth order ( $N^4\text{LO}$ ) [4–7] and even beyond [8]. The available versions of the  $N^4\text{LO}$  potentials differ from each other, among other things, in the functional form of the regulator function: while the interactions of Ref. [6] are regularized with a nonlocal cutoff, local regularization in coordinate (momentum) space is employed for pion-exchange contributions in Ref. [5] (Ref. [7]). As demonstrated in Refs. [7,9], the employed types of local regulators do not, per construction, affect the long-range part of the interaction, thus generating a smaller amount of finite-cutoff artifacts. For a related discussion of regulator artifacts in uniform matter see Refs. [10,11]. The resulting  $N^4\text{LO}^+$  potentials of Ref. [7] lead to the description of the 2013 Granada database [12] for neutron-proton and proton-proton scattering below  $E_{\text{lab}} = 300$  MeV, which is comparable to or even better than that based on the phenomenological high-precision potentials such as the AV18 [13], CDBonn [14], Nijm1, and Nijm2 [15] models, featuring at the same time a much smaller number of adjustable parameters. We also

mention recent efforts towards constructing the  $NN$  [16–18] and three-nucleon [19,20] potentials using the heavy-baryon formulation of chiral EFT with explicit  $\Delta(1232)$  degrees of freedom.

In Refs. [21–23], we have applied the semilocal coordinate-space regularized (SCS) chiral  $NN$  potentials of Refs. [5,9] to analyze nucleon-deuteron ( $Nd$ ) scattering along with selected properties of light- and medium-mass nuclei. For similar studies of nuclear matter properties, selected electroweak processes, and nucleon-deuteron radiative capture reactions see Refs. [24], [25], and [26], respectively. All these calculations are based on the  $NN$  forces only and thus can only be regarded as complete at leading order (LO) and next-to-leading order (NLO) in the chiral expansion. In fact, our main motivation in these studies was to analyze the convergence pattern of chiral EFT, estimate the achievable accuracy at various orders, and identify promising observables to look for three-nucleon force (3NF) effects and/or meson-exchange-current contributions. To estimate the truncation error of the chiral expansion, we followed the algorithm formulated in Ref. [9] and modified appropriately to account for missing 3NFs and meson-exchange currents. For the interpretation, validation, and further developments of this approach to uncertainty quantification in a Bayesian framework see Refs. [27,28], while the robustness of this method and possible alternatives are discussed in Ref. [23].

One important outcome of these studies is the observation that many  $Nd$  scattering observables at intermediate energies as well as the energies and radii of light and medium-mass nuclei calculated with  $NN$  forces only show significant deviations from experimental data, whose magnitude matches well with the expected size of  $3NF$  contributions in the Weinberg power counting scheme.

In this paper we perform, for the first time, *complete* calculations of few- and many-nucleon systems at third order of the chiral expansion, i.e., at  $N^2LO$ , utilizing semilocal coordinate-space regulators [5,9,21,23]. We explore different ways to fix the low-energy constants (LECs)  $c_D$  and  $c_E$  in the three-nucleon sector and show that they can be determined from the  $^3H$  binding energy and the differential cross section minimum in elastic  $Nd$  scattering at intermediate energies. This allows us to make parameter-free predictions for  $A > 3$  systems. We provide a comparison of the complete  $N^2LO$  results with results at LO and NLO and estimate truncation errors. More details regarding the calculations will be presented in separate publications [29] for  $p$ -shell nuclei and [30] for  $Nd$  scattering.

Our paper is organized as follows. In Sec. II we specify the regularized expressions of the chiral  $3NF$  at  $N^2LO$  and discuss the determination of the LECs  $c_D$  and  $c_E$ . Section III is devoted to  $Nd$  elastic scattering, while our predictions for ground state and excitation energies for  $p$ -shell nuclei are reported in Secs. IV and V, respectively. Finally, the main results of our study are summarized in Sec. VI.

## II. DETERMINATION OF $c_D$ AND $c_E$

The  $N^2LO$  three-nucleon force in momentum space is given by

$$\begin{aligned}
V^{3N} = & \frac{g_A^2}{8F_\pi^4} \frac{\vec{\sigma}_1 \cdot \vec{q}_1 \vec{\sigma}_3 \cdot \vec{q}_3}{[q_1^2 + M_\pi^2][q_3^2 + M_\pi^2]} \\
& \times [\boldsymbol{\tau}_1 \cdot \boldsymbol{\tau}_3 (-4c_1 M_\pi^2 + 2c_3 \vec{q}_1 \cdot \vec{q}_3) \\
& + c_4 \boldsymbol{\tau}_1 \times \boldsymbol{\tau}_3 \cdot \boldsymbol{\tau}_2 \vec{q}_1 \times \vec{q}_3 \cdot \vec{\sigma}_2] \\
& - \frac{g_A D}{8F_\pi^2} \frac{\vec{\sigma}_3 \cdot \vec{q}_3}{q_3^2 + M_\pi^2} \boldsymbol{\tau}_1 \cdot \boldsymbol{\tau}_3 \vec{\sigma}_1 \cdot \vec{q}_3 \\
& + \frac{1}{2} E \boldsymbol{\tau}_1 \cdot \boldsymbol{\tau}_2 + 5 \text{ permutations}, \quad (1)
\end{aligned}$$

where the subscripts refer to the nucleon labels and  $\vec{q}_i = \vec{p}_i' - \vec{p}_i$ , with  $\vec{p}_i'$  and  $\vec{p}_i$  being the final and initial momenta of the nucleon  $i$ . Furthermore,  $q_i \equiv |\vec{q}_i|$ ,  $\sigma_i$  and  $\boldsymbol{\tau}_i$  are the Pauli spin and isospin matrices, respectively, and  $c_i$ ,  $D$ , and  $E$  denote the corresponding LECs while  $g_A$  and  $F_\pi$  refer to the nucleon axial coupling and pion decay constant. Throughout this work, we use the same values for the subleading pion-nucleon LECs  $c_i$  as employed in the  $NN$  forces of Ref. [9], namely,  $c_1 = -0.81 \text{ GeV}^{-1}$ ,  $c_3 = -4.69 \text{ GeV}^{-1}$ , and  $c_4 = 3.40 \text{ GeV}^{-1}$ . These are compatible with the recent determinations from the Roy-Steiner analysis [31]. The values of the LECs accompanying the  $NN$  contact interactions can be provided by the authors upon request. We also apply the same regularization procedure to the  $3NF$  as used in the employed  $NN$  potentials.

Specifically, regularization of the  $2\pi$ -exchange  $3NF$  is carried out by Fourier-transforming the expressions into coordinate space (see Eq. (2.11) of Ref. [32]) and subsequently multiplying them with the regulator functions used in Ref. [9]:

$$\begin{aligned}
V_{2\pi}^{3N}(\vec{r}_{12}, \vec{r}_{32}) \longrightarrow & V_{2\pi}^{3N}(\vec{r}_{12}, \vec{r}_{32}) \left[ 1 - \exp\left(-\frac{r_{12}^2}{R^2}\right) \right]^6 \\
& \times \left[ 1 - \exp\left(-\frac{r_{32}^2}{R^2}\right) \right]^6. \quad (2)
\end{aligned}$$

Here,  $\vec{r}_{ij}$  denotes the relative distance between the nucleons  $i$  and  $j$ . For the one-pion-exchange-contact  $3NF$  term proportional to the LEC  $D$  in Eq. (1), a similar procedure is employed to regularize the singular behavior with respect to the momentum transfer  $\vec{q}_3$ . In addition, following Ref. [9], the contact interaction between nucleons 1 and 2 is regularized by multiplying the momentum-space matrix elements with a nonlocal Gaussian regulator  $\exp(-(p_{12}^2 + p'_{12}{}^2)/\Lambda^2)$ , where  $\vec{p}_{12} = (\vec{p}_1 - \vec{p}_2)/2$ ,  $\vec{p}'_{12} = (\vec{p}'_1 - \vec{p}'_2)/2$  and  $\Lambda = 2R^{-1}$ . Finally, for the purely contact interaction proportional to the LEC  $E$ , we apply a nonlocal regulator in momentum space,

$$\begin{aligned}
V_{\text{cont}}^{3N} \longrightarrow & V_{\text{cont}}^{3N} \exp\left(-\frac{4p_{12}^2 + 3k_3^2}{4\Lambda^2}\right) \\
& \times \exp\left(-\frac{4p'_{12}{}^2 + 3k_3'^2}{4\Lambda^2}\right), \quad (3)
\end{aligned}$$

where  $\vec{k}_3 = 2(\vec{p}_3 - (\vec{p}_1 + \vec{p}_2)/2)/3$  and  $\vec{k}_3' = 2(\vec{p}'_3 - (\vec{p}'_1 + \vec{p}'_2)/2)/3$  are the corresponding Jacobi momenta. The numerical implementation of the regularization in the partial wave basis will be detailed in a separate publication. We verified the correctness of the implementation by comparing two independent calculations of matrix elements of the  $3NF$ .

The three-nucleon force at  $N^2LO$  involves two LECs which govern the strength of the one-pion-exchange-contact and purely contact  $3NF$  contributions and cannot be fixed from nucleon-nucleon scattering. Here and in what follows, we use the notation of Ref. [33] and express these LECs in terms of the dimensionless parameters  $c_D$  and  $c_E$  via

$$D = \frac{c_D}{F_\pi^2 \Lambda_\chi}, \quad E = \frac{c_E}{F_\pi^4 \Lambda_\chi}, \quad (4)$$

employing the value of  $\Lambda_\chi = 700 \text{ MeV} \simeq M_\rho$  for the chiral-symmetry breaking scale. The determination of  $c_D$  and  $c_E$  requires at least two few- or many-nucleon low-energy observables. In this analysis we utilize a commonly adopted practice [33–37] and regard the  $^3H$  binding energy as one such observable. Employing this constraint by solving the Faddeev equations establishes a relation between the two LECs as visualized in Fig. 1 for the regulator choices of  $R = 0.9 \text{ fm}$  and  $R = 1.0 \text{ fm}$ , which leaves us with a single yet undetermined parameter  $c_D$ . Notice that when calculating the  $^3H$  binding energy to determine  $c_E$  as a function of  $c_D$ , we have taken into account the electromagnetic interaction between two neutrons as implemented in the AV18 potential [13]. However, the results presented in Secs. IV and V are based on the point-Coulomb interaction only. This small inconsistency is irrelevant at the accuracy level of our study.

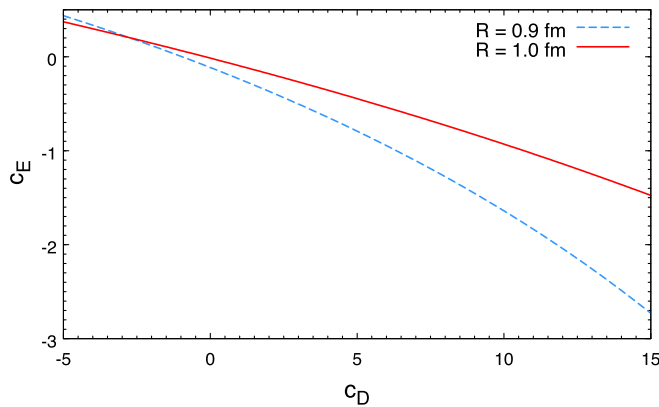


FIG. 1. Correlation between the LECs  $c_D$  and  $c_E$  induced by the requirement to reproduce the  ${}^3\text{H}$  binding energy for the cutoff choices of  $R = 0.9$  fm (blue dashed line) and  $R = 1.0$  fm (red solid line).

A wide range of observables has been considered in the literature to constrain the remaining LEC. These include the neutron-deuteron doublet scattering length  ${}^2a$  [33,37], triton  $\beta$  decay [36], the  ${}^4\text{He}$  binding energy [34], the point-proton radii of  ${}^3\text{H}$  and/or  ${}^4\text{He}$ , and selected properties of few-nucleon systems [35,38]. We also mention the approach of Ref. [39] to perform a global fit of LECs entering the two- and three-nucleon forces to  $NN$  scattering data in combination with few- and many-nucleon observables. In this paper we explore several possibilities for fixing  $c_D$  based solely on the nucleon-deuteron ( $Nd$ ) experimental data. Such a procedure has an advantage of being insensitive to the four-nucleon force and exchange currents, which may affect observables in heavier systems and reactions involving electroweak probes, and gives us the opportunity to make predictions for nuclei with  $A \geq 4$ . Given that we only consider the leading contribution to the  $3NF$  at  $N^2\text{LO}$ , we do not use  $Nd$  polarization observables to determine the  $c_D/c_E$  values and restrict ourselves to the differential and total cross sections and  ${}^2a$ . Specifically, the differential cross section for elastic  $Nd$  scattering around its minimum at energies of  $E_N \sim 50$  MeV and above<sup>1</sup> is well known to be sensitive to the  $3NF$  contributions [40,41].

In Fig. 2 we show the constraints on  $c_D$  resulting from the reproduction of the proton-deuteron differential cross section data at  $E_N = 70$  and 135 MeV of Ref. [42] and  $E_N = 108$  MeV of Ref. [43] for  $\theta_{c.m.} \sim 128^\circ$  (using a single experimental point). Notice that there is a discrepancy between the data of Ref. [42] and the Kernfysisch Versneller Instituut (KVI) measurement of the differential cross section at  $E_N = 135$  MeV of Ref. [44]. We also show constraints emerging from the reproduction of the (derived) neutron-deuteron total cross section data of Ref. [45] at the same energies and the experimental value of  ${}^2a = 0.645 \pm 0.008$  fm of Ref. [46]. In all calculations, the LEC  $c_E$  is set to reproduce the  ${}^3\text{H}$  binding

energy according to the correlation shown in Fig. 1. Notice further that we do not include the Coulomb interactions in our  $Nd$  scattering calculations. The effect of the Coulomb interaction in the cross section for the considered kinematics is below the statistical and systematic uncertainties of our analysis [47,48]. We further emphasize that our scattering calculations are carried out including  $NN$  partial waves up to  $j_{\text{max}} = 5$  and using a standard approximate treatment of the isospin  $T = 3/2$  channels (see Sec. III for further information on the partial wave truncation and Ref. [40] for more details). This is sufficient to obtain converged results for observables under consideration. We also neglect isospin  $T = 3/2$  components of the  $3NF$  when calculating  $Nd$  scattering observables, which are insignificant for the observables we consider [49].

As shown in Fig. 2, the strongest constraint on  $c_D$  results from the cross section minimum at the lowest considered energy of  $E_N = 70$  MeV. While the differential cross section data at  $E_N = 135$  MeV have the same statistical and systematic errors, the significantly larger truncation error at this energy leads to a less precise determination of  $c_D$ . It is also interesting to see that the doublet scattering length  ${}^2a$ , whose experimental value is known to a high accuracy of  $\sim 1\%$ , does not constrain  $c_D$  at  $N^2\text{LO}$ . This is in line with the known strong correlation between  ${}^2a$  and the  ${}^3\text{H}$  binding energy (the so-called Phillips line [50]; see also Ref. [36] for a similar conclusion). Notice, however, that electromagnetic interactions between the nucleons are known to have a sizable effect on  ${}^2a$  [51]. Thus, a more complete treatment of the electromagnetic interaction may affect the position of the central value of  $c_D$  extracted from this observable. Performing a  $\chi^2$  fit to all considered observables by taking into account the experimental statistical and systematic as well as the theoretical truncation errors added in quadrature, we obtain the values of  $c_D = 1.7 \pm 0.8$  for  $R = 0.9$  fm and  $c_D = 7.2 \pm 0.7$  for  $R = 1.0$  fm. The listed uncertainties for  $c_D$  are estimates of the standard deviations. When including the data only up to 108 MeV, the resulting  $c_D$  values read  $c_D = 2.1 \pm 0.9$  for  $R = 0.9$  fm and  $c_D = 7.2 \pm 0.9$  for  $R = 1.0$  fm. The corresponding  $c_E$  values are  $c_E = -0.329^{+0.103}_{-0.106}$  ( $c_E = -0.381^{+0.117}_{-0.122}$ ) for  $R = 0.9$  fm and  $c_E = -0.652 \pm 0.067$  ( $c_E = -0.652^{+0.086}_{-0.087}$ ) for  $R = 1.0$  fm using experimental data up to 135 MeV (up to 108 MeV). We emphasize that the simplistic procedure for estimating the central values and uncertainties of the LECs  $c_D$  and  $c_E$  adopted in this study does not take into account the statistical and systematic errors of the nuclear potentials. In future calculations at higher chiral orders, a more sophisticated approach to error analysis along the lines of Refs. [7,52] should be employed.

It is important to address the question of robustness of our approach to determine the constants  $c_D$  and  $c_E$  with respect to the choice of data used in the fits. To this end, we performed fits to the  $Nd$  differential cross section data in a wider range of center-of-mass (c.m.) angles. In Fig. 3 we show the resulting description of the data along with the corresponding  $\chi^2$  as a function of  $c_D$  for the already mentioned  $pd$  data at  $E = 70$  MeV [42] (30 data points), 108 MeV [43] (16 data points), and 135 MeV [42] (21 data points). The actual calculations were performed for  $R = 0.9$  fm using five different  $c_D$  values, namely,  $c_D = -2.0, 0.0, 2.0, 4.0,$  and  $6.0$ . In all cases, the  $c_E$

<sup>1</sup>At low energy, the minimum in the differential cross section becomes less pronounced due to the  $s$ -wave dominance, and the sensitivity to the  $3NF$  decreases.

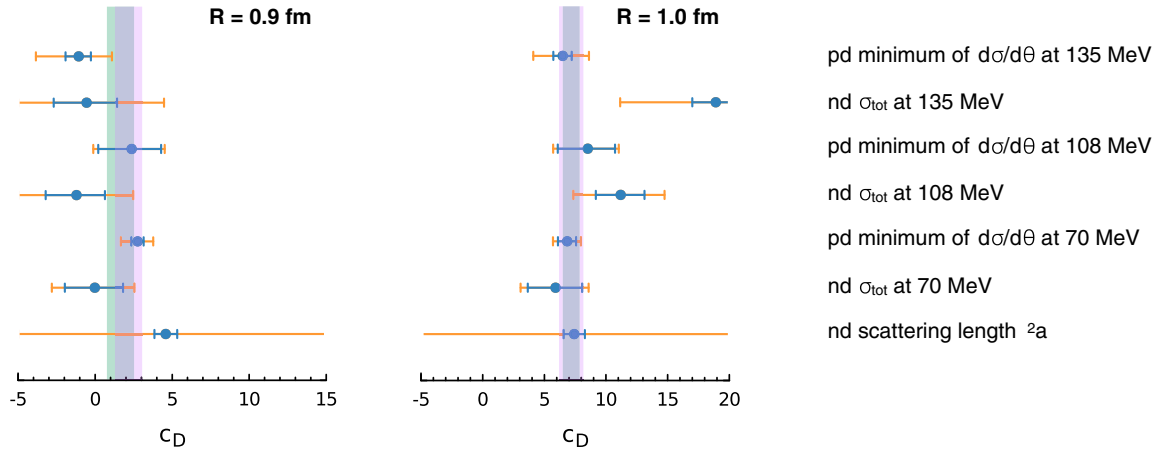


FIG. 2. Determination of the LEC  $c_D$  from the differential cross section in elastic  $pd$  scattering, total  $nd$  cross section, and the  $nd$  doublet scattering length  $^2a$  for the cutoff choices of  $R = 0.9$  fm and  $R = 1.0$  fm. The smaller (blue) error bars correspond to the experimental statistical and systematic uncertainties added in quadrature. The larger (orange) error bars also take into account the truncation error estimated as described in Ref. [21] and added in quadrature. The green (violet) bands show standard error intervals of  $c_D$  resulting from a combined least squares single-parameter fit to all observables (to observables up to  $E_N = 108$  MeV) using the orange error bars.

values are taken from the correlation line shown in Fig. 1. The shown  $\chi^2$  does not take into account the estimated theoretical uncertainty of our calculations. Notice further that in all cases, we have taken into account the systematic errors in addition to the statistical ones as given in Refs. [42,44]. While the resulting  $c_D$  values at 70 and 108 MeV are close to each other and also to the central value of  $c_D \sim 2.1$  from the global fit up to 108 MeV quoted above, the fit to the  $E = 135$  MeV data prefers a value of  $c_D \sim -0.7$ . However, taking into account the relatively large truncation uncertainty at  $E = 135$  MeV, the extracted values of  $c_D$  at all three energies are still compatible with each other (see the left-hand graphs of Fig. 2 and left-hand panels of Fig. 3).

### III. $Nd$ SCATTERING

We are now in the position to discuss our predictions for nucleon-deuteron ( $Nd$ ) scattering observables. To this aim, we calculate a  $3N$  scattering operator  $T$  by solving the Faddeev-type integral equation [40,53–55] in a partial wave momentum-space basis. Throughout this section, we restrict ourselves to the harder regulator value of  $R = 0.9$  fm in order to cover a broader kinematical range up to  $E_{\text{lab}} = 250$  MeV and focus on a very restricted set of observables.<sup>2</sup> A more detailed discussion of  $Nd$  elastic and breakup scattering at  $N^2\text{LO}$  will be published elsewhere. Since we are going to compare our  $3N$  scattering predictions with  $pd$  data, we have replaced the neutron-neutron ( $nn$ ) components of the  $NN$  potential with the corresponding proton-proton ( $pp$ ) ones (with the Coulomb force being subtracted). Furthermore, in order to provide converged results, we have solved the  $3N$

Faddeev equations by taking into account all partial wave states with the  $2N$  total angular momenta up to  $j_{\text{max}} = 5$  and  $3N$  total angular momenta up to  $J_{\text{max}} = 25/2$ . The  $3NF$  was included up to  $J_{\text{max}} = 7/2$ .

At low energies, the most interesting observable is the analyzing power  $A_y$  for  $nd$  elastic scattering with polarized neutrons. Theoretical predictions of the phenomenological high-precision  $NN$  potentials such as the AV18 [13], CDBonn [14], Nijm1, and Nijm2 [15] fail to explain the experimental data for  $A_y$  as visualized in Fig. 4. The data are underestimated by  $\approx 30\%$  in the region of the  $A_y$  maximum which corresponds to the c.m. angles of  $\Theta_{\text{c.m.}} \approx 125^\circ$ . Combining these  $NN$  potentials with the  $2\pi$ -exchange TM99  $3NF$  model [57] removes approximately only half of the discrepancy to the data (see Fig. 4). That effect is, however, model dependent: if the Urbana IX  $3NF$  model [58] is used instead of the TM99  $3NF$ , one observes practically no effects on  $A_y$  (see the left-hand panel of Fig. 4). The predictions for the  $A_y$  based on the chiral  $NN$  potentials appear to be similar to those of phenomenological models (see Ref. [23] and references therein). Combining the  $N^2\text{LO}$  SCS chiral potential with the  $N^2\text{LO}$   $3NF$  only slightly improves the description of  $A_y$ . The behavior is qualitatively similar to the one observed for the TM99  $3NF$ , but the effect is approximately two times smaller in magnitude. As expected, the theoretical predictions appear to be quite insensitive to the actual value of  $c_D$  as visualized by a rather narrow magenta band in the right-hand panel of Fig. 4, which corresponds to the variation of  $c_D = -2.0, \dots, 6.0$ . In fact, this observable is well known to be very sensitive only to  $^3P_j$   $NN$  force components [59], while both  $3NF$  contact interactions act predominantly in the  $s$  waves. However, the truncation error at  $N^2\text{LO}$  is rather large and, in fact, comparable in magnitude with the observed deviation between the predictions and experimental data. It would be interesting to see whether the  $A_y$  puzzle would persist upon inclusion of higher-order corrections to the  $3NF$  (see Refs. [60,61] for recent work along this line and Ref. [62]

<sup>2</sup>The results for low-energy scattering observables using  $R = 1.0$  fm are comparable to the ones using  $R = 0.9$  fm (see also Ref. [23] for a similar conclusion for calculations based on  $NN$  forces only). More details are given in a separate publication [30].



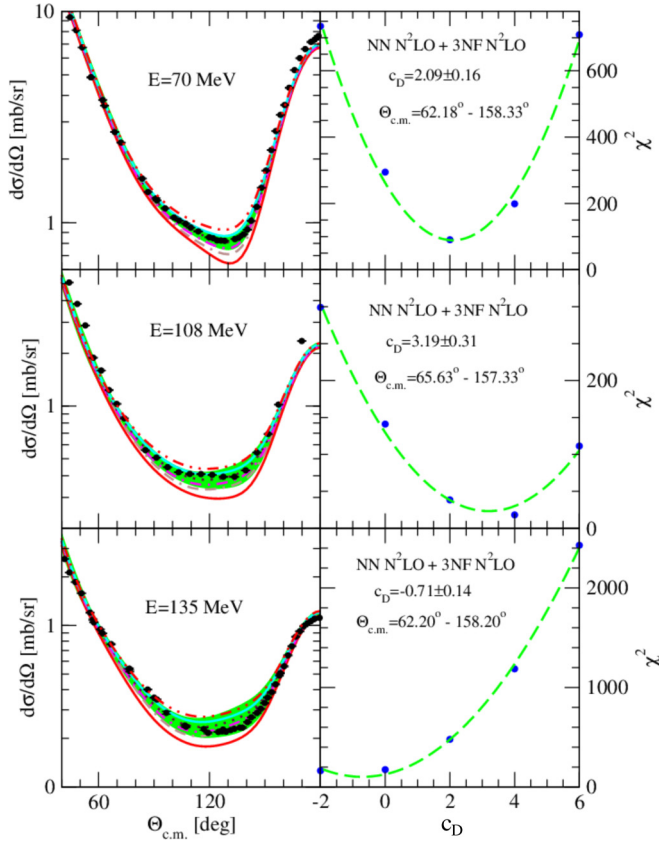


FIG. 3. The  $nd$  elastic scattering cross section at the incoming neutron laboratory energies  $E = 70, 108,$  and  $135$  MeV. Left: Solid (red) lines are predictions of the  $N^2LO$  SCS  $NN$  potential with the regulator  $R = 0.9$  fm. Combining this  $NN$  potential with the  $N^2LO$  3NF using five different  $(c_D, c_E)$  combinations leads to results shown by the (brown) double-dash-dotted, (magenta) dash-dotted, (maroon) dotted, (cyan) solid, and (red) double-dot-dashed lines for  $c_D = -2.0, 0.0, 2.0, 4.0,$  and  $6.0$ , respectively. The (green) bands show the estimated truncation error of predictions at  $N^2LO$  with  $c_D = 2.0$ . The corresponding  $c_E$  values are in all cases taken from the correlation line shown in Fig. 1. The (black) dots depict  $pd$  data from Ref. [42] at  $E = 70$  and  $E = 135$  MeV and from Ref. [43] at  $E = 108$  MeV. Right: The  $\chi^2$  fits to the experimental data in the indicated angular regions based on these five pairs of  $(c_D, c_E)$  values are shown by dashed (green) lines. The legends in the right-hand panel provide the best fit  $c_D$  values to the data at each laboratory energy over the indicated angular range.

for a related discussion in the framework of pionless EFT). As for other  $Nd$  elastic scattering observables at low energy, we found the effects of the chiral 3NF at  $N^2LO$  to be rather small, and the good description of the data, already reported in Ref. [21] for the calculations based on the  $NN$  forces, remains intact after inclusion of the 3NF.

At intermediate energies, the effects of the 3NF start to become more pronounced. In particular, as already discussed in Sec. II, the differential cross section is significantly underestimated in the minimum region when calculated based on  $NN$  forces only. The same pattern is observed in calculations based on the high-precision phenomenological potentials as

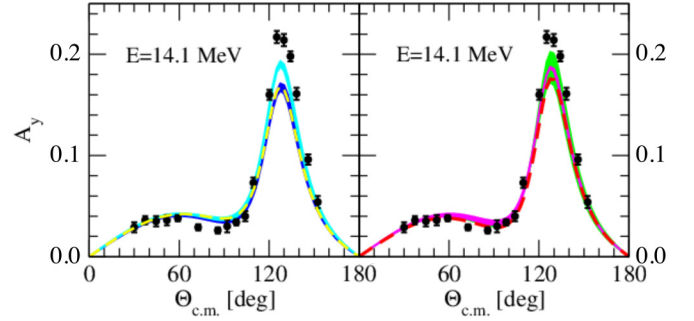


FIG. 4. The neutron analyzing power  $A_y$  in  $nd$  elastic scattering at  $E_n = 14.1$  MeV. Left: The predictions based on the phenomenological  $NN$  potentials AV18, CD Bonn, Nijm1, and Nijm2 alone (blue band) or in combination with the TM99 3NFs (cyan band). The dashed (yellow) line is the result based on the AV18  $NN$  potential in combination with the Urbana IX 3NF. Right: The dashed (red) line is the prediction of the  $N^2LO$  SCS  $NN$  potential with the regulator  $R = 0.9$  fm. The (magenta) band covers the predictions obtained with this  $N^2LO$   $NN$  potential combined with the  $N^2LO$  3NF using  $c_D = -2.0, \dots, 6.0$  (and the corresponding  $c_E$  values fixed from the correlation line). The (green) band gives the estimated truncation error at  $N^2LO$  for the value of  $c_D = 2.0$ . The (black) dots depict  $pd$  data from Ref. [56].

well. The improved description of  $Nd$  elastic scattering cross section data up to about 130 MeV upon inclusion of the  $N^2LO$  3NF resembles the situation found in calculations based on phenomenological 3NFs [41,63] such as the TM99 [57] and Urbana IX [58] models. However, the inclusion of the available 3NFs has so far not provided an explanation of the growing discrepancies between the cross section data and theoretical predictions at larger energies and backward angles as exemplified in Fig. 5 for  $E_N = 250$  MeV. The astonishing similarity of the predictions based on phenomenological models and chiral interactions can presumably be traced back to the fact that the basic mechanism underlying these 3NFs is the  $2\pi$  exchange. It is also interesting to observe that the  $N^2LO$  theoretical predictions are rather insensitive to the variation of  $c_D$  and  $c_E$ . Clearly, the convergence of the chiral expansion at

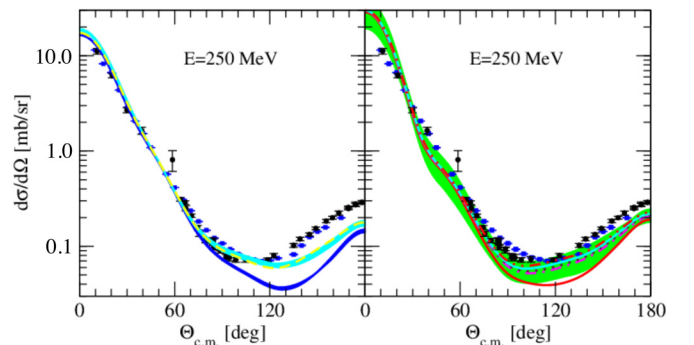


FIG. 5. The  $nd$  elastic scattering cross section at  $E_n = 250$  MeV. The lines and bands in the left-hand (right-hand) panel are the same as in the left-hand (left-hand) panel of Fig. 4 (Fig. 3). (Black) dots depict the  $pd$  data from Ref. [64] while (blue) squares are  $nd$  data from Ref. [65].

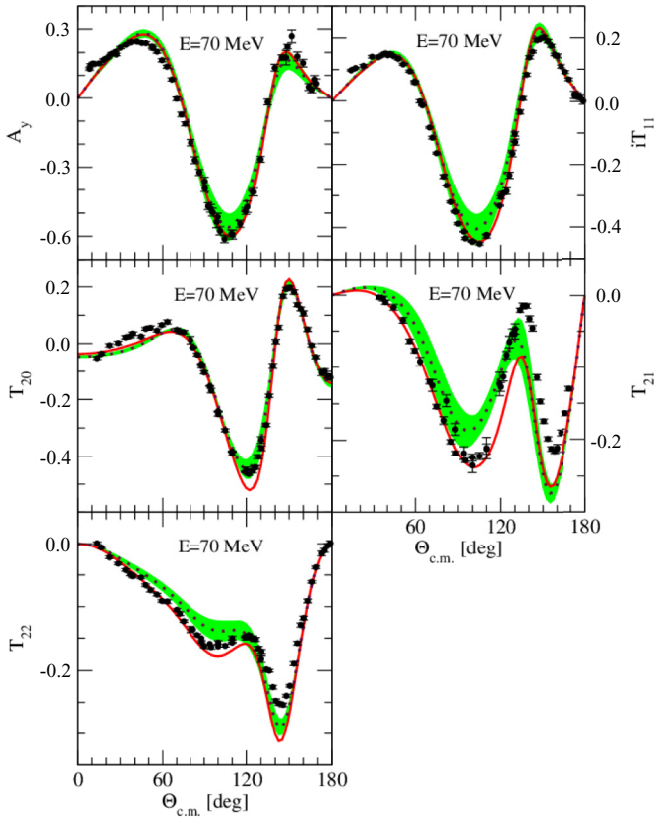


FIG. 6. The  $nd$  elastic scattering neutron ( $A_y$ ) and deuteron ( $iT_{11}$ ) vector analyzing powers as well as deuteron tensor analyzing powers  $T_{20}$ ,  $T_{21}$ , and  $T_{22}$  at the incoming neutron laboratory energy  $E = 70$  MeV. The solid red lines are predictions of the  $N^2$ LO SCS  $NN$  potential with the regulator  $R = 0.9$  fm. Combining that  $NN$  potential with  $N^2$ LO  $3NF$  with strengths of the contact terms ( $c_D = 2.0$ ,  $c_E = -0.3446$ ) leads to results shown by the dotted maroon lines with their estimated truncation error depicted by the green bands. The black dots depict  $pd$  data for  $A_y$  at  $E = 65$  MeV from Ref. [66] and for other analyzing powers at  $E = 70$  MeV from Ref. [42].

such high energies is expected to be rather slow as reflected by the broad error band in the right-hand panel of this figure. In fact, given the truncation uncertainty of our  $N^2$ LO results, the description of the experimental data appears to be adequate at this chiral order.

Finally, as a representative example, we show in Fig. 6 our predictions for the complete set of analyzing powers at  $E = 70$  MeV together with the estimated truncation errors. Except for the tensor analyzing power  $T_{21}$  at backward angles, we observe a reasonably good description of the data given the uncertainty of our results. Clearly, one will have to go to higher chiral orders in order to improve the accuracy of the calculations and to perform more quantitative tests of the theory. Work along these lines is in progress.

#### IV. GROUND STATE ENERGIES FOR $p$ -SHELL NUCLEI

For  $p$ -shell nuclei, we use no-core configuration interaction (NCCI) methods to solve the many-body Schrödinger

equation. These methods have advanced rapidly in recent years and one can now accurately solve fundamental problems in nuclear structure and reaction physics using realistic interactions (see, e.g., Ref. [67] and references therein). Here we follow Refs. [68,69] where, for a given interaction, we diagonalize the resulting many-body Hamiltonian in a sequence of truncated harmonic-oscillator (HO) basis spaces. The goal is to achieve convergence as indicated by independence of the basis parameters, but in practice we use extrapolations to estimate the binding energy in the complete (infinite-dimensional) space [68,70–73]. Specifically, we employ the same extrapolation method as in Refs. [23,69] with extrapolation uncertainty estimates following Ref. [69]. These NCCI calculations were performed on the Cray XC30 Edison and Cray XC40 Cori at NERSC and the IBM BG/Q Mira at Argonne National Laboratory, using the code MFDN [74–76].

To improve the convergence behavior of the bound state calculations we employ the similarity renormalization group (SRG) [77–80] approach that provides a straightforward and flexible framework for consistently evolving (softening) the Hamiltonian and other operators, including three-nucleon interactions [81–84]. In the presence of explicit  $3NF$ s, this additional softening of the chiral interaction is necessary in order to obtain sufficiently converged results on current supercomputers for  $p$ -shell nuclei. The flow equation for the three-body system is solved using a HO Jacobi-coordinate basis [84]. The SRG evolution and subsequent transformation to single-particle coordinates were performed on a single node using an efficient OPENMP parallelized code.

As a consequence of the softening of the interaction, our results may depend on the SRG parameter  $\alpha$ , because we do not incorporate any induced interactions beyond  $3NF$ s. Without explicit  $3NF$ s, this dependence appears to be negligible (see Fig. 7): for  ${}^4\text{He}$  the results with and without SRG evolution are within about 10 keV of each other, and for  ${}^{12}\text{C}$  the difference between the ground state energies at  $\alpha = 0.04$  and  $\alpha = 0.08 \text{ fm}^4$  is significantly less than the estimated extrapolation uncertainty. Once we add explicit  $3NF$ s to the  $NN$  potential we find that the results for  ${}^4\text{He}$  do depend on the SRG parameter, and that this dependence increases as we evolve the interaction further ( $\alpha = 0$  corresponds to the interaction without SRG). However, for  $A \geq 6$  this dependence becomes of the same order as (or smaller than) our extrapolation uncertainty estimate. We can combine the extrapolation uncertainty and the SRG dependence (estimated by taking the difference between the binding energies at  $\alpha = 0.04$  and  $\alpha = 0.08 \text{ fm}^4$ ) into a single numerical uncertainty estimate, treating them as independent.

In Fig. 7 we also see that the binding energies depend in a nontrivial way on the values of  $c_D$  and  $c_E$ . In particular, as we increase  $c_D$  (and change the corresponding  $c_E$  accordingly) the ground state energy of  ${}^4\text{He}$  increases, whereas that of  ${}^{12}\text{C}$  decreases with increasing  $c_D$ . It turns out that for  $A = 6$  and 7 the binding energy is nearly independent (within our numerical uncertainty estimates) of the actual value of  $c_D$ , whereas starting from  $A = 8$  we do see a systematic decrease of the ground state energy with increasing  $c_D$ , at least for  $R = 1.0$  fm and values of  $c_D$  between 2 and 8 [29]. Furthermore,

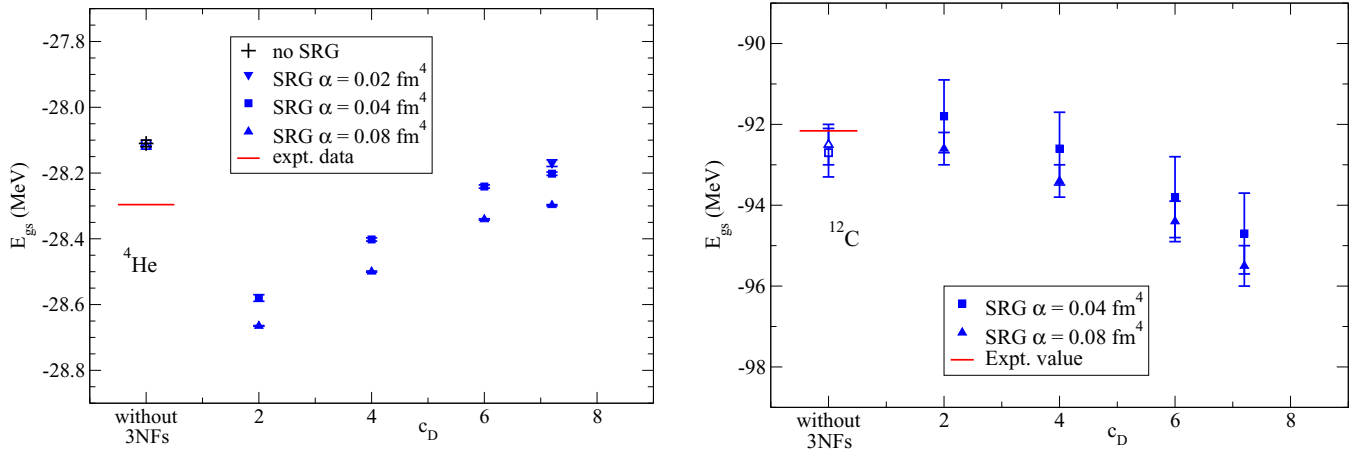


FIG. 7. Extrapolated ground state energy for  ${}^4\text{He}$  (left) and  ${}^{12}\text{C}$  (right) using chiral  $\text{N}^2\text{LO}$  interactions with regulator  $R = 1.0$  fm, and SRG evolution parameters  $\alpha = 0.02, 0.04$ , and  $0.08$  fm $^4$ , with and without explicit 3NFs. The error bars correspond to the extrapolation uncertainty estimates only.

this dependence on  $c_D$  seems to be stronger as one moves away from  $N = Z$ .

We have visualized our results for the ground state energies of  $A = 4$ – $12$  nuclei in Fig. 8, for the regulator of  $R = 1.0$  fm. The results at  $\text{N}^2\text{LO}$  are all obtained with the preferred values of  $c_D = 7.2$  and  $c_E = -0.671$  for the LECs, and an SRG parameter of  $\alpha = 0.08$  fm $^4$ . The open blue symbols correspond to *incomplete* calculations at  $\text{N}^2\text{LO}$  using  $NN$ -only

interactions (with induced 3NFs), whereas the complete  $\text{N}^2\text{LO}$  calculations including 3NFs are shown by solid symbols. For comparison, we have also included the results at LO and NLO with  $R = 1.0$  fm. For  $A = 4$ – $9$  these calculations at LO and NLO were performed without SRG evolution [23]; the results for  $A = 10, 11, 12$ , and  ${}^{16}\text{O}$  in Fig. 8 are for an SRG parameter of  $\alpha = 0.08$  fm $^4$ , and include induced 3NFs. (Note that at LO and NLO there are no 3NFs.)

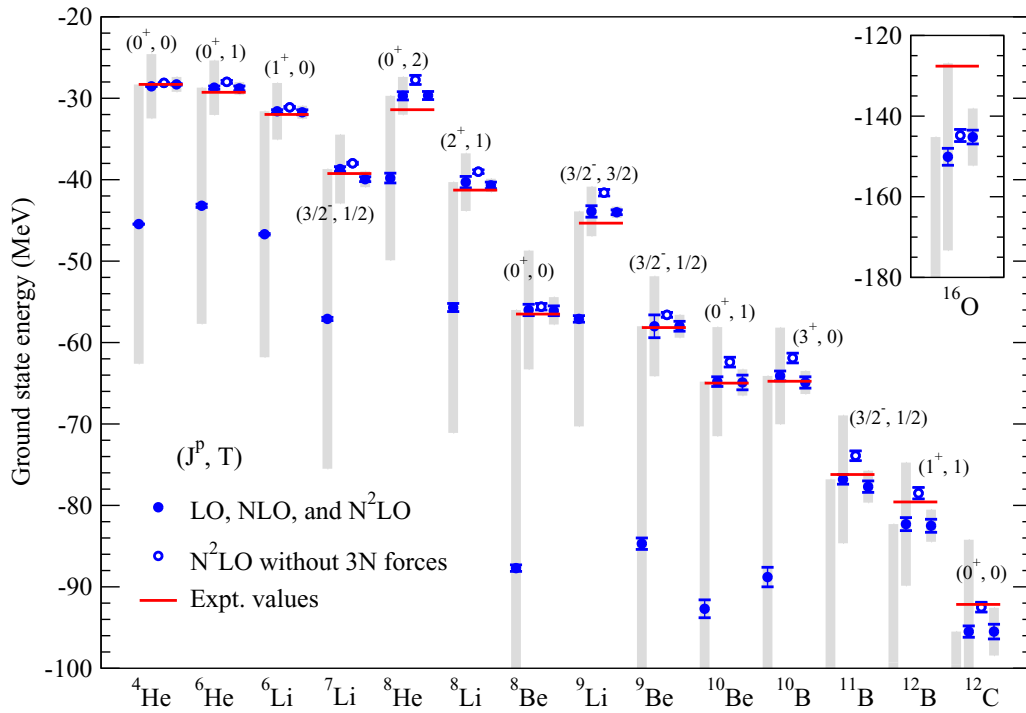


FIG. 8. Calculated ground state energies in MeV using chiral LO, NLO, and  $\text{N}^2\text{LO}$  interactions at  $R = 1.0$  fm (blue symbols) in comparison with experimental values (red levels). For each nucleus the LO, NLO, and  $\text{N}^2\text{LO}$  results are the left, middle, and right symbols and bars, respectively. The open blue symbols correspond to incomplete calculations at  $\text{N}^2\text{LO}$  using  $NN$ -only interactions. Blue error bars indicate the NCCI extrapolation uncertainty and, where applicable, an estimate of the SRG dependence. The shaded bars indicate the estimated truncation error at each chiral order following Ref. [21]. Note that the LO results for  $A = 11, 12$ , and for  ${}^{16}\text{O}$  are off the scale, but (part of) the corresponding shaded uncertainty bar is included.

TABLE I. Extrapolated binding energies of  $A = 6$ – $12$  nuclei in MeV, as well as  ${}^4\text{He}$  and  ${}^{16}\text{O}$ , with the chiral interactions at  $\text{N}^2\text{LO}$  using semilocal coordinate-space regulators, as well as SRG evolution to improve numerical convergence of the many-body calculations. For the LEC  $c_D$ , we use the values of  $c_D = 2.1$  for  $R = 0.9$  fm and  $c_D = 7.2$  for  $R = 1.0$  fm. The uncertainty estimate is only the extrapolation uncertainty in the many-body calculation, and does not include any SRG uncertainty, the chiral truncation error, or any uncertainty due to uncertainties in the LECs.

Nucleus	$J^P$	$N_{\text{max}}$	$\alpha$ (fm $^4$ )	$R = 0.9$ fm		$R = 1.0$ fm		Expt.
				$NN + 3NF_{\text{induced}}$	$NN + 3NF$	$NN + 3NF_{\text{induced}}$	$NN + 3NF$	
${}^4\text{He}$	$0^+$	14	0.04	$27.231 \pm 0.006$	$28.425 \pm 0.004$	$28.113 \pm 0.006$	$28.202 \pm 0.005$	28.296
			0.08	$27.233 \pm 0.002$	$28.502 \pm 0.002$	$27.119 \pm 0.001$	$28.298 \pm 0.002$	
${}^6\text{He}$	$0^+$	12	0.04	$27.00 \pm 0.16$	$28.73 \pm 0.15$	$27.88 \pm 0.15$	$28.55 \pm 0.15$	29.27
			0.08	$27.10 \pm 0.10$	$28.94 \pm 0.08$	$27.99 \pm 0.14$	$28.79 \pm 0.08$	
${}^6\text{Li}$	$1^+$	12	0.04	$30.15 \pm 0.15$	$31.79 \pm 0.18$	$31.02 \pm 0.13$	$31.49 \pm 0.16$	31.99
			0.08	$30.24 \pm 0.07$	$32.00 \pm 0.07$	$31.12 \pm 0.08$	$31.72 \pm 0.06$	
${}^7\text{Li}$	$\frac{3}{2}^-$	10	0.04	$36.89 \pm 0.25$	$39.04 \pm 0.30$	$37.91 \pm 0.20$	$38.66 \pm 0.28$	39.24
			0.08	$36.92 \pm 0.12$	$39.19 \pm 0.14$	$37.99 \pm 0.11$	$38.94 \pm 0.14$	
${}^8\text{He}$	$0^+$	10	0.04	$26.9 \pm 1.0$	$29.6 \pm 0.5$	$27.5 \pm 0.4$	$29.3 \pm 0.4$	31.41
			0.08	$26.87 \pm 0.4$	$29.88 \pm 0.4$	$27.75 \pm 0.5$	$29.66 \pm 0.4$	
${}^8\text{Li}$	$2^+$	10	0.04	$37.87 \pm 0.3$	$40.85 \pm 0.4$	$38.92 \pm 0.3$	$40.38 \pm 0.4$	41.28
			0.08	$37.90 \pm 0.15$	$41.07 \pm 0.25$	$39.02 \pm 0.2$	$40.70 \pm 0.2$	
${}^8\text{Be}$	$0^+$	10	0.04	$53.7 \pm 0.3$	$56.2 \pm 0.5$	$55.4 \pm 0.4$	$55.6 \pm 0.5$	56.50
			0.08	$53.8 \pm 0.2$	$56.6 \pm 0.3$	$55.6 \pm 0.3$	$56.1 \pm 0.3$	
${}^9\text{Li}$	$\frac{3}{2}^-$	10	0.04	$40.5 \pm 0.4$	$44.1 \pm 0.4$	$41.6 \pm 0.4$	$43.9 \pm 0.4$	45.34
			0.08	$40.44 \pm 0.2$	$44.50 \pm 0.2$	$41.63 \pm 0.3$	$44.04 \pm 0.2$	
${}^9\text{Be}$	$\frac{3}{2}^-$	10	0.04	$54.8 \pm 0.4$	$57.8 \pm 0.5$	$56.5 \pm 0.4$	$57.5 \pm 0.5$	58.16
			0.08	$54.81 \pm 0.2$	$58.42 \pm 0.25$	$56.57 \pm 0.2$	$58.04 \pm 0.25$	
${}^{10}\text{Be}$	$0^+$	8	0.08	$60.4 \pm 0.5$	$65.6 \pm 0.5$	$62.4 \pm 0.5$	$64.9 \pm 0.5$	64.98
${}^{10}\text{B}$	$3^+$	8	0.08	$60.0 \pm 0.5$	$66.0 \pm 0.5$	$61.9 \pm 0.5$	$64.9 \pm 0.5$	64.75
${}^{11}\text{B}$	$\frac{3}{2}^-$	8	0.08	$71.7 \pm 0.5$	$78.8 \pm 0.5$	$73.9 \pm 0.5$	$77.7 \pm 0.5$	76.21
${}^{12}\text{B}$	$1^+$	8	0.08	$76.2 \pm 0.5$	$83.7 \pm 0.6$	$78.5 \pm 0.6$	$82.5 \pm 0.5$	79.58
${}^{12}\text{C}$	$0^+$	8	0.08	$89.7 \pm 0.4$	$96.9 \pm 0.5$	$92.5 \pm 0.5$	$95.5 \pm 0.5$	92.16
${}^{16}\text{O}$	$0^+$	8	0.08	$139.8 \pm 0.6$	$146.9 \pm 0.8$	$144.8 \pm 0.6$	$145.2 \pm 0.8$	127.62

For all  $A = 4$ – $12$  nuclei the ground state energies decrease when we add the  $3NF$ s with the preferred LECs to the  $NN$  interaction at  $\text{N}^2\text{LO}$  (see Fig. 8). For  ${}^4\text{He}$  this decrease is very small, but for  $A = 6$  and larger this decrease is at least half an MeV, growing to a decrease of about 3 MeV in the ground state energy of  ${}^{12}\text{C}$ . Up to  $A = 10$  the ground state energies with the  $3NF$ s are significantly closer to their experimental values than without; however, for  $A = 12$  the decrease of the ground state energies moves them further away from the experimental value. In contrast, for  ${}^{16}\text{O}$  (see the inset in Fig. 8) the binding energy at  $\text{N}^2\text{LO}$  is, within the numerical uncertainties, the same with or without  $3NF$ s, and significantly below the experimental value.

We also show the chiral truncation error estimate for these ground state energies following Refs. [5,9,21,23]. To be specific, following this method implies that the chiral error estimate at LO is, in practice, determined by  $\delta E^{(0)} = \max(|E^{(2)} - E^{(0)}|, |E^{(3)} - E^{(0)}|)$ , and at NLO and  $\text{N}^2\text{LO}$  by  $Q\delta E^{(0)}$  and  $Q^2\delta E^{(0)}$ , respectively, where  $Q$  is the chiral expansion parameter. Up to  $A = 9$  we use  $Q = M_\pi/\Lambda_b \approx 0.23$ , but for  $A = 10$  and above the average relative momentum scale of the nucleons inside the nucleus increases, to about 185 MeV for  ${}^{16}\text{O}$ , corresponding to  $Q \approx 0.3$  [23]. (It turns out that the chiral error estimate with  $3NF$ s included at  $\text{N}^2\text{LO}$  is up to about 10% smaller than those without  $3NF$ s for  $A = 6$ – $12$ .)

For most of the 15 nuclei in Fig. 8, our complete results at  $\text{N}^2\text{LO}$  agree, to within the chiral error estimate, with the experimental values; the exceptions are  ${}^8\text{He}$ ,  ${}^9\text{Li}$ ,  ${}^{12}\text{B}$ ,  ${}^{12}\text{C}$ , and  ${}^{16}\text{O}$ . Both  ${}^8\text{He}$  and  ${}^9\text{Li}$  are slightly underbound in our calculations; they are also both weakly bound and neutron rich. Small changes in either the two-neutron force or the three-neutron force (neither of which are very well constrained experimentally) could potentially have significant effects on these neutron-rich nuclei. In this respect it is also interesting to note that the effect of the  $3NF$ s is noticeably larger for  ${}^8\text{He}$  and  ${}^9\text{Li}$  than for  ${}^8\text{Be}$  and  ${}^9\text{Be}$ . However,  ${}^{16}\text{O}$  is noticeably overbound at  $\text{N}^2\text{LO}$ , with or without  $3NF$ s (see also Ref. [85] for a related discussion in the context of nuclear lattice simulations). This overbinding starts at  $A = 12$ , where, with  $3NF$ s, both  ${}^{12}\text{B}$  and  ${}^{12}\text{C}$  are overbound, with the experimental value only slightly outside the chiral truncation error estimate, and seems to be systematic for the heavier nuclei.

Table I gives our calculated results at  $\text{N}^2\text{LO}$  for both  $R = 0.9$  fm and  $R = 1.0$  fm. Although the qualitative behavior is similar for the two regulator values, that is, the explicit  $3NF$ s at  $\text{N}^2\text{LO}$  decrease the ground state energy for all  $A = 6$ – $12$  nuclei, the additional binding from these  $3NF$ s is significantly larger at  $R = 0.9$  fm than at  $R = 1.0$  fm. For both regulator values the additional binding from the  $3NF$ s leads to a better agreement with the data up to about



$A = 10$  or  $11$ . Furthermore, the regulator dependence is noticeably smaller with the  $3NF$ s included than without these contributions.

However, inclusion of the  $3NF$ s leads to a noticeable overbinding for both  $^{12}\text{B}$  and  $^{12}\text{C}$ , whereas the effect of the  $3NF$ s is surprisingly small for  $^{16}\text{O}$ , and does not move the  $^{16}\text{O}$  binding energy any closer to experiment. Note that a smaller value of  $c_D$  would give better agreement with the experimental binding energy for  $^{12}\text{C}$ : with values of  $c_D = 2.0$  and  $c_E = -0.193$  for the LECs using  $R = 1.0$  fm, the ground state energy of  $^{12}\text{C}$  is in perfect agreement with its experimental value (see Fig 7).

It is interesting to compare our results to similar calculations using different versions of the chiral interactions. Our  $\text{N}^2\text{LO}$  results for the ground state energies of  $p$ -shell nuclei are in a qualitative agreement with the Green's function Monte Carlo calculations reported in Ref. [37] and based on the local  $NN$  potentials with explicit  $\Delta$  contributions to the two-pion exchange, accompanied with the locally regularized  $3NF$  at  $\text{N}^2\text{LO}$ . In particular, the ground state energy of  $^{12}\text{C}$ , the heaviest nucleus considered in that work, appears to be slightly overbound at  $\text{N}^2\text{LO}$ . It is, however, difficult to make a more quantitative comparison since the authors of that paper do not show results at lower chiral orders and at  $\text{N}^2\text{LO}$  using  $NN$  interactions only. Also no estimation of the truncation errors is provided. Another local version of the chiral  $NN$  interaction, constructed in Refs. [86,87] and accompanied with the locally regularized  $3NF$  at  $\text{N}^2\text{LO}$ , was employed in Refs. [88,89] to calculate properties of nuclei up to  $A = 16$  using the auxiliary field diffusion Monte Carlo methods. This interaction leads to similar results at LO, showing typically a strong overbinding for all nuclei. The NLO local forces used in Refs. [88,89], however, turn out to be considerably more repulsive than the semilocal interactions employed in our analysis, which results in underbinding for most of the considered nuclei. Still, their NLO results are consistent with ours and with experimental data within errors. At  $\text{N}^2\text{LO}$ , the authors of Refs. [88,89] do not provide results based on the  $NN$  interactions only, leaving no possibility to quantify  $3NF$  effects in their scheme. It is furthermore found in Ref. [88] that, while being equivalent modulo higher-order terms, different operator choices of the contact  $3NF$  at  $\text{N}^2\text{LO}$  may induce large differences for the  $^{16}\text{O}$  binding energy for (very) soft cutoff values. This indicates that subleading short-range  $3NF$  contributions may play an important role, especially for soft choices of the regulator. The description of the ground state energies of nuclei up to  $A = 16$  reported in Ref. [89] at  $\text{N}^2\text{LO}$  is comparable to ours, but the results for  $^{12}\text{C}$  and  $^{16}\text{O}$  show the opposite trend of being underbound. We further emphasize that the short-range part of the  $3NF$  was constrained in that paper in the  $A = 5$  system using experimental data on  $n$ - $\alpha$  scattering, while all results of our calculations for  $A \geq 4$  are parameter-free predictions. Finally, it is interesting to compare our results for  $^4\text{He}$ ,  $^8\text{He}$ , and  $^{16}\text{O}$  with those reported in Ref. [18] using chiral EFT with explicit  $\Delta(1232)$  degrees of freedom. For a momentum cutoff  $\Lambda = 450$  MeV, the corresponding ground state energies at  $\Delta\text{NNLO}$  are found in Ref. [18] to be

$E(^4\text{He}) = -28.29(0.78)$  MeV,<sup>3</sup>  $E(^8\text{He}) = -27.0$  MeV, and  $E(^{16}\text{O}) = -117.0(1.8)$  MeV with the estimated truncation errors given in parentheses. The truncation error for  $^8\text{He}$  is not quoted in Ref. [18]. These numbers are to be compared with our predictions for  $R = 1.0$  fm and  $\alpha = 0.8$  at the same chiral order, namely,  $E(^4\text{He}) = -28.3(0.9)$  MeV,  $E(^8\text{He}) = -29.7(0.5)$  MeV, and  $E(^{16}\text{O}) = -145.2(7.1)$  MeV, where we only quote the estimated truncation errors, and the corresponding experimental values of  $-28.296$ ,  $-31.41$ , and  $-127.62$  MeV, respectively. The most pronounced difference is observed for the ground state energy of  $^{16}\text{O}$ , for which the  $\Delta$ -full approach yields almost 30 MeV less binding. Still, given the different employed regularization schemes and fitting protocols, it is difficult to draw unambiguous conclusions on the role of the  $\Delta$  isobar based on such a comparison.

We also calculated the point-proton radius of  $^4\text{He}$  by solving the Faddeev-Yakubovsky equations. The obtained values are  $r_p^{\text{LO}} = 1.008$  fm,  $r_p^{\text{NLO}} = 1.420$  fm, and  $r_p^{\text{N}^2\text{LO}} = 1.434$  fm for  $R = 0.9$  fm while  $r_p^{\text{LO}} = 1.064$  fm,  $r_p^{\text{NLO}} = 1.390$  fm, and  $r_p^{\text{N}^2\text{LO}} = 1.443$  fm for the softer cutoff choice of  $R = 1.0$  fm. Using the algorithm of Ref. [23] for estimating the truncation error, our final results at  $\text{N}^2\text{LO}$  are  $r_p^{\text{N}^2\text{LO}} = 1.434 \pm 0.022$  fm for  $R = 0.9$  fm and  $r_p^{\text{N}^2\text{LO}} = 1.443 \pm 0.018$  fm for  $R = 1.0$  fm. Our predictions are thus barely consistent (within errors) with the empirical value of  $r_p = 1.462(6)$  fm [90] while in somewhat better agreement with the empirical value  $1.457(10)$  fm deduced in Ref. [91]. In future studies, we plan to extend these calculations to heavier nuclei and higher chiral orders.

## V. EXCITATION ENERGIES FOR $p$ -SHELL NUCLEI

In Fig. 9 we present our results for the excitation energies for selected states of  $A = 6$ – $12$  nuclei, at  $\text{N}^2\text{LO}$  with  $R = 1.0$  fm, first without explicit  $3NF$ s (open blue symbols), then with explicit  $3NF$ s using the preferred values of  $c_D = 7.2$  and  $c_E = -0.671$  for the LECs (solid blue symbols), and followed by the experimental values. All of the shown results were obtained in the largest achievable basis space in the  $N_{\text{max}}$  truncation, and for a fixed SRG parameter of  $\alpha = 0.08$  fm<sup>4</sup> and fixed HO basis parameter of  $\hbar\omega = 20$  MeV. We include the maximum of the difference between our results at  $\hbar\omega = 20$  MeV and those at  $\hbar\omega = 16$  MeV or  $\hbar\omega = 24$  MeV as a rough estimate of the numerical uncertainty of our calculations.

The results clearly show that including the  $3NF$ s moves the excitation energies for most of these states closer to the experimental values. There are only two significant exceptions, both for  $A = 12$ : the lowest  $2^+$  state of  $^{12}\text{B}$  and the lowest  $1^+$  state of  $^{12}\text{C}$ . Both of these two states are in better agreement with experiment without  $3NF$ s than with the  $3NF$ s, and for both, including the  $3NF$ s lowers the excitation energies significantly.

In  $^{12}\text{B}$  we actually find that the lowest  $2^+$  state becomes the ground state when the  $3NF$ s are included, at almost 1 MeV

<sup>3</sup>The  $\alpha$ -particle binding energy was used as input in the determination of the LECs entering the  $3NF$  in Ref. [18].

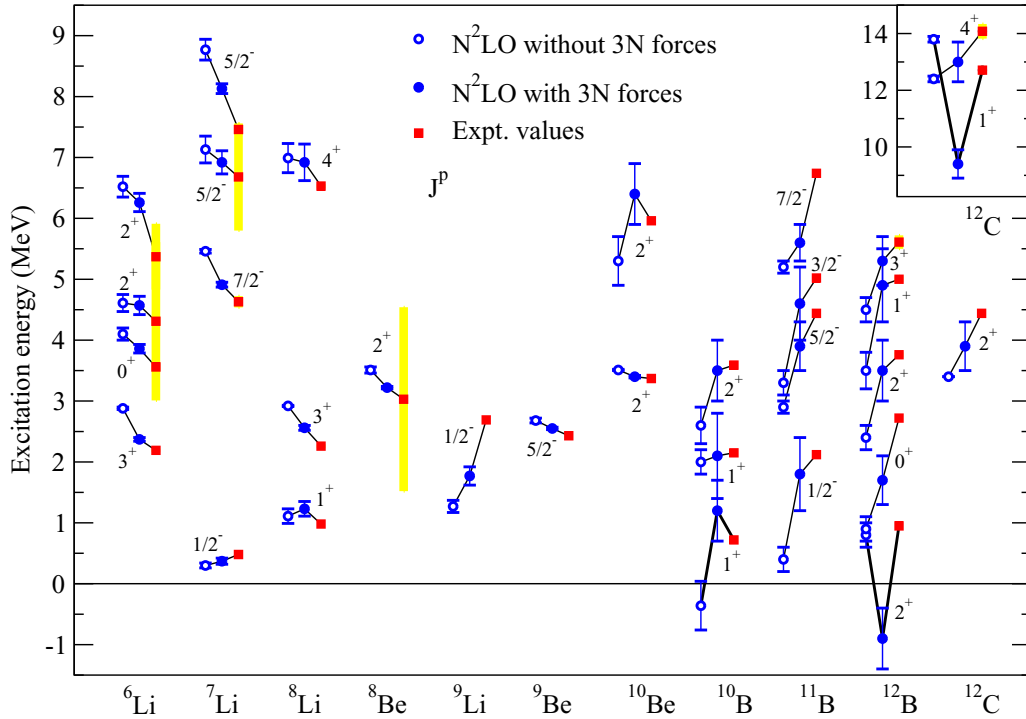


FIG. 9. Calculated excitation energies in MeV using chiral  $N^2LO$  at  $R = 1.0$  fm with and without explicit  $3NFs$  for a fixed SRG parameter of  $\alpha = 0.08$  fm<sup>4</sup> and fixed HO basis parameter of  $\hbar\omega = 20$  MeV. Results are presented as open blue circles for calculations without explicit  $3NFs$ , solid blue dots for calculations including  $3NFs$  using  $c_D = 7.2$ , and red squares for experimental values. The yellow bars are the experimental width of broad resonances. We define an “uncertainty range” for our calculations by the maximum of the difference between calculations at  $\hbar\omega = 20$  MeV and those at  $\hbar\omega = 16$  MeV or  $\hbar\omega = 24$  MeV.

below the actual  $1^+$  ground state. From Fig. 8 we can see that also the  $1^+$  ground state becomes more deeply bound when the  $3NFs$  are included, but the additional binding from the  $3NFs$  is apparently stronger for the lowest  $2^+$  state than for the lowest  $1^+$  state. In contrast, the excitation energies of the other excited states of  $^{12}B$  increase when the  $3NFs$  are included, and move considerably closer to their experimental values.

The excitation energy of the lowest  $1^+$  state of  $^{12}C$  (with  $T = 0$ ; the analog state of the ground state of  $^{12}B$  is around 15 MeV, in agreement with experiment) drops by about 4 MeV when the  $3NFs$  are included, from about 14 MeV to below 10 MeV, whereas the experimental value is at 12.7 MeV. We find a similar dependence of this state on the  $3NFs$  using the regulator  $R = 0.9$  fm, and also with the Entem-Machleidt chiral  $N^3LO$   $NN$  potential plus  $N^2LO$   $3NFs$  [92,93]. Of course, our calculations are not converged, and in particular for  $^{12}C$  it is known that the first excited  $0^+$  state (the Hoyle state) cannot be represented in the finite HO bases that we are employing in our calculations, and is indeed absent from the low-lying spectrum in our calculations in basis spaces up to  $N_{max} = 10$ . It is possible that this  $1^+$  state is also sensitive to configurations that are beyond  $N_{max} = 10$ , whereas the  $2^+$  and  $4^+$  excited states are rotational excitations of the ground state and having a similar structure as the ground state and, therefore, converge at similar rates as the ground state.

In the case of  $^{10}B$  we find the now-accepted result of obtaining a  $1^+$  ground state without  $3NFs$  [94] instead of the observed  $3^+$  ground state. When we include consistent  $3NFs$ ,

we do obtain a  $3^+$  ground state in concert with experiment, as may be expected [35]. The excitation energies of the two additional  $^{10}B$  states shown in Fig. 9, the second  $1^+$  state and a  $2^+$  state, move closer to experiment with the addition of the  $3NFs$  as well. However, the two low-lying  $1^+$  states exhibit a strong mixing [83], which results in a large basis space dependence for these two states, as well as sensitivity to the SRG parameter, preventing us from reliably extracting their excitation energies.

Although these three states are sensitive to the LECs  $c_D$  and  $c_E$ , we do find a qualitatively similar effect if we change  $c_D$  over a range from 2 to 8 [29]. However, a lower value of  $c_D$  would improve the agreement with experiment for the  $1^+$  state of  $^{12}C$  and the  $2^+$  state of  $^{12}B$ : with  $c_D = 2.0$  and  $c_E = -0.193$  the  $2^+$  state of  $^{12}B$  becomes essentially degenerate with the  $1^+$  ground state, and the excitation energy of the  $1^+$  state of  $^{12}C$  becomes about 11.2 MeV, that is, significantly closer to the experimental value. For  $^{10}B$  the situation is much more complicated, due to the strong mixing between the lowest two  $1^+$  states as a function of the basis truncation parameters  $N_{max}$  and  $\hbar\omega$  [83]. Note, however, that none of these excitation energies is very well converged. The excitation energies of most of the other states shown here are significantly less sensitive to the LECs.

Another interesting observation is that for  $A = 6, 7$ , and 8 the inclusion of the  $3NFs$  tends to reduce the excitation energies, whereas for  $A = 10, 11$ , and 12 the inclusion of the  $3NFs$  tends to increase the excitation energies (with the

exception of the aforementioned three states). Furthermore, both tendencies move the excitation energies closer to their experimental values. Nevertheless, even with the 3NFs included, the calculated excitation energies tend to be too large for  $A = 6, 7$ , and  $8$  (i.e., the spectrum is too spread out), whereas for  $A = 11$  and  $12$  they tend to be too small (i.e., the spectrum is too compressed).

## VI. SUMMARY AND OUTLOOK

In this paper we applied the SCS  $N^2$ LO chiral  $NN$  potential combined with the  $N^2$ LO 3NF, regularized in the same way, to selected properties of few- and many-nucleon systems up to  $A = 16$ . The main findings of our study can be summarized as follows:

- (i) We explored the possibility to determine the LECs  $c_D$  and  $c_E$  from a range of observables in the 3N system. To this aim we first computed numerically the LECs  $c_E$  as a function of  $c_D$  from the requirement that the  $^3\text{H}$  binding energy is correctly reproduced. To fix the value of  $c_D$  we calculated the  $Nd$  doublet scattering length as well as the differential and total cross sections in  $Nd$  scattering at various energies. By taking into account the estimated truncation error at  $N^2$ LO, we found the  $Nd$  doublet scattering length to yield only very weak constraints on the allowed  $c_D$  values. These findings support the conclusions of Ref. [36] and can be traced back to the strong correlation between this observable and the  $^3\text{H}$  binding energy known as the Phillips line [50]. From the considered 3N observables, the strongest constraint on the  $c_D$  values is found to emerge from the precise experimental data of Ref. [42] for the differential cross section at  $E_N = 70$  MeV in its minimum region. The constraints on the LEC  $c_D$  placed by all considered observables appear to be mutually consistent within errors with the only exception of the total cross section at  $E_N = 135$  MeV for the softer cutoff of  $R = 1.0$  fm. A global analysis of all considered scattering observables is shown to allow for a precise determination of the LEC  $c_D$  for both considered cutoff values.
- (ii) The resulting nuclear Hamiltonian at  $N^2$ LO was applied to a selected range of other observables in elastic  $Nd$  scattering. For the low-energy nucleon analyzing power  $A_y$ , the application of consistent chiral interactions supports earlier findings based on the phenomenological  $NN$  potentials accompanied by the TM99 3NF; however, the resulting effects are smaller in magnitude by a factor of  $\sim 2$ . We also looked at various spin observables at  $E_N = 70$  MeV, which turn out to be reasonably well described given the estimated truncation errors at this order. At higher energies the discrepancies between the calculated observables and experimental data increase, but it is difficult to draw definite conclusions due to rather large truncation errors at this chiral order.
- (iii) Using NCCI methods, we studied the ground state and low-lying excitation energies of  $p$ -shell nuclei. For

almost all considered cases with very few exceptions such as, e.g., the  $A = 12$  nuclei, adding the consistent 3NF to the  $NN$  interaction is found to significantly improve the description of experimental data. The predicted ground state energies of  $p$ -shell nuclei show a good agreement with the data except for  $^{16}\text{O}$ , which appears to be overbound.

To summarize, we obtain very promising results for a broad range of few- and many-nucleon observables at  $N^2$ LO of the chiral expansion. In the future, we plan to extend these studies beyond this chiral order [32,95–102] (see Refs. [61,103] for first steps along these lines, which will allow us to improve the accuracy of our predictions and perform more stringent tests of the theoretical framework). Notice, however, that the coordinate-space regularization of the 3NF and its subsequent partial wave decomposition represent highly nontrivial tasks starting from  $N^3$ LO. Fortunately, this major obstacle can now be overcome thanks to the newest momentum-space version of the local regulator employed in the currently most precise version of the chiral  $NN$  potentials of Ref. [7]. Work along these lines is in progress.

## ACKNOWLEDGMENTS

This study was performed within the Low Energy Nuclear Physics International Collaboration (LENPIC) project and was supported by BMBF (Contracts No. 05P15PCFN1 and No. 05P15RDFN1 - NUSTAR.DA), by the European Community-Research Infrastructure Integrating Activity “Study of Strongly Interacting Matter” (acronym Hadron-Physics3, Grant Agreement No. 2) under the Seventh Framework Programme of EU, the ERC project 307986 STRONGINT, by the DFG (SFB 1245), by DFG and NSFC (CRC 110, Grants No. TRR110 and No. 11621131001), by the Polish National Science Centre under Grants No. 2016/22/M/ST2/00173 and No. 2016/21/D/ST2/01120, by the Chinese Academy of Sciences (CAS) Presidents International Fellowship Initiative (PIFI) (Grant No. 2018DM0034), by the U.S. Department of Energy (DOE) under Grants No. DE-FG02-87ER40371, No. DE-SC0015376 (DOE Topical Collaboration in Nuclear Theory for Double-Beta Decay and Fundamental Symmetries) and No. DE-SC0018223 (SciDAC-4/NUCLEI) and by Volkswagen-Stiftung (Grant No. 93562). Numerical calculations were performed on the supercomputer cluster of the JSC, Jülich, and the Lichtenberg high-performance cluster at the TU Darmstadt, Germany. Numerical calculations were also performed at the Argonne Leadership Computing Facility, which is a DOE Office of Science User Facility supported under Contract No. DE-AC02-06CH11357 with resources provided by an INCITE award, Nuclear Structure and Nuclear Reactions, from the U.S. DOE Office of Advanced Scientific Computing. This research also used computational resources provided by the National Energy Research Scientific Computing Center (NERSC), which is supported by the U.S. DOE Office of Science.

- [1] E. Epelbaum, H. W. Hammer, and U.-G. Meißner, *Rev. Mod. Phys.* **81**, 1773 (2009).
- [2] R. Machleidt and D. R. Entem, *Phys. Rep.* **503**, 1 (2011).
- [3] E. Epelbaum and U.-G. Meißner, *Annu. Rev. Nucl. Part. Sci.* **62**, 159 (2012).
- [4] D. R. Entem, N. Kaiser, R. Machleidt, and Y. Nosyk, *Phys. Rev. C* **91**, 014002 (2015).
- [5] E. Epelbaum, H. Krebs, and U.-G. Meißner, *Phys. Rev. Lett.* **115**, 122301 (2015).
- [6] D. R. Entem, R. Machleidt, and Y. Nosyk, *Phys. Rev. C* **96**, 024004 (2017).
- [7] P. Reinert, H. Krebs, and E. Epelbaum, *Eur. Phys. J. A* **54**, 86 (2018).
- [8] D. R. Entem, N. Kaiser, R. Machleidt, and Y. Nosyk, *Phys. Rev. C* **92**, 064001 (2015).
- [9] E. Epelbaum, H. Krebs, and U.-G. Meißner, *Eur. Phys. J. A* **51**, 53 (2015).
- [10] I. Tews, S. Gandolfi, A. Gezerlis, and A. Schwenk, *Phys. Rev. C* **93**, 024305 (2016).
- [11] A. Dyhdalo, R. J. Furnstahl, K. Hebeler, and I. Tews, *Phys. Rev. C* **94**, 034001 (2016).
- [12] R. Navarro Pérez, J. E. Amaro, and E. Ruiz Arriola, *Phys. Rev. C* **88**, 024002 (2013); **88**, 069902(E) (2013).
- [13] R. B. Wiringa, V. G. J. Stoks, and R. Schiavilla, *Phys. Rev. C* **51**, 38 (1995).
- [14] R. Machleidt, *Phys. Rev. C* **63**, 024001 (2001).
- [15] V. G. J. Stoks, R. A. M. Klomp, C. P. F. Terheggen, and J. J. deSwart, *Phys. Rev. C* **49**, 2950 (1994).
- [16] M. Piarulli, L. Girlanda, R. Schiavilla, R. N. Pérez, J. E. Amaro, and E. R. Arriola, *Phys. Rev. C* **91**, 024003 (2015).
- [17] M. Piarulli, L. Girlanda, R. Schiavilla, A. Kievsky, A. Lovato, L. E. Marcucci, S. C. Pieper, M. Viviani, and R. B. Wiringa, *Phys. Rev. C* **94**, 054007 (2016).
- [18] A. Ekström, G. Hagen, T. D. Morris, T. Papenbrock, and P. D. Schwartz, *Phys. Rev. C* **97**, 024332 (2018).
- [19] E. Epelbaum, H. Krebs, and U.-G. Meißner, *Nucl. Phys. A* **806**, 65 (2008).
- [20] H. Krebs, A. M. Gasparyan, and E. Epelbaum, *Phys. Rev. C* **98**, 014003 (2018).
- [21] S. Binder, A. Calci, E. Epelbaum, R. J. Furnstahl, J. Golak, K. Hebeler, H. Kamada, H. Krebs, J. Langhammer, S. Liebig, P. Maris, Ulf-G. Meißner, D. Minossi, A. Nogga, H. Potter, R. Roth, R. Skibiński, K. Topolnicki, J. P. Vary, and H. Witała (LENPIC Collaboration), *Phys. Rev. C* **93**, 044002 (2016).
- [22] P. Maris *et al.*, *EPJ Web Conf.* **113**, 04015 (2016).
- [23] S. Binder, A. Calci, E. Epelbaum, R. J. Furnstahl, J. Golak, K. Hebeler, T. Huther, H. Kamada, H. Krebs, P. Maris, Ulf-G. Meißner, A. Nogga, R. Roth, R. Skibiński, K. Topolnicki, J. P. Vary, K. Vobig, and H. Witała (LENPIC Collaboration), *Phys. Rev. C* **98**, 014002 (2018).
- [24] J. Hu, Y. Zhang, E. Epelbaum, Ulf-G. Meißner, and J. Meng, *Phys. Rev. C* **96**, 034307 (2017).
- [25] R. Skibiński, J. Golak, K. Topolnicki, H. Witała, E. Epelbaum, H. Krebs, H. Kamada, Ulf-G. Meißner, and A. Nogga, *Phys. Rev. C* **93**, 064002 (2016).
- [26] R. Skibiński *et al.*, *Few-Body Syst.* **58**, 28 (2017).
- [27] R. J. Furnstahl, N. Klco, D. R. Phillips, and S. Wesolowski, *Phys. Rev. C* **92**, 024005 (2015).
- [28] J. A. Melendez, S. Wesolowski, and R. J. Furnstahl, *Phys. Rev. C* **96**, 024003 (2017).
- [29] P. Maris *et al.* (unpublished).
- [30] H. Witała *et al.*, *Few-Body Syst.* (to be published).
- [31] M. Hoferichter, J. Ruiz de Elvira, B. Kubis, and Ulf-G. Meißner, *Phys. Rev. Lett.* **115**, 192301 (2015).
- [32] V. Bernard, E. Epelbaum, H. Krebs, and Ulf-G. Meißner, *Phys. Rev. C* **77**, 064004 (2008).
- [33] E. Epelbaum, A. Nogga, W. Glöckle, H. Kamada, Ulf-G. Meißner, and H. Witała, *Phys. Rev. C* **66**, 064001 (2002).
- [34] A. Nogga, P. Navrátil, B. R. Barrett, and J. P. Vary, *Phys. Rev. C* **73**, 064002 (2006).
- [35] P. Navrátil, V. G. Gueorguiev, J. P. Vary, W. E. Ormand, and A. Nogga, *Phys. Rev. Lett.* **99**, 042501 (2007).
- [36] D. Gazit, S. Quaglioni, and P. Navrátil, *Phys. Rev. Lett.* **103**, 102502 (2009).
- [37] M. Piarulli, A. Baroni, L. Girlanda, A. Kievsky, A. Lovato, E. Lusk, L. E. Marcucci, S. C. Pieper, R. Schiavilla, M. Viviani, and R. B. Wiringa, *Phys. Rev. Lett.* **120**, 052503 (2018).
- [38] J. E. Lynn, I. Tews, J. Carlson, S. Gandolfi, A. Gezerlis, K. E. Schmidt, and A. Schwenk, *Phys. Rev. C* **96**, 054007 (2017).
- [39] A. Ekström, G. R. Jansen, K. A. Wendt, G. Hagen, T. Papenbrock, B. D. Carlsson, C. Forssén, M. Hjorth-Jensen, P. Navrátil, and W. Nazarewicz, *Phys. Rev. C* **91**, 051301 (2015).
- [40] W. Glöckle, H. Witała, D. Hüber, H. Kamada, and J. Golak, *Phys. Rep.* **274**, 107 (1996).
- [41] H. Witała, W. Glöckle, D. Hüber, J. Golak, and H. Kamada, *Phys. Rev. Lett.* **81**, 1183 (1998).
- [42] K. Sekiguchi, H. Sakai, H. Witała, W. Glöckle, J. Golak, M. Hatano, H. Kamada, H. Kato, Y. Maeda, J. Nishikawa, A. Nogga, T. Ohnishi, H. Okamura, N. Sakamoto, S. Sakoda, Y. Satou, K. Suda, A. Tamii, T. Uesaka, T. Wakasa, and K. Yako, *Phys. Rev. C* **65**, 034003 (2002).
- [43] K. Ermisch, H. R. Amir-Ahmadi, A. M. van den Berg, R. Castelijns, B. Davids, E. Epelbaum, E. VanGarderen, W. Glöckle, J. Golak, M. N. Harakeh, M. Hunyadi, M. A. de Huu, N. Kalantar-Nayestanaki, H. Kamada, M. Kis, M. Mahjour-Shafiei, A. Nogga, R. Skibiński, H. Witała, and H. J. Wörtche, *Phys. Rev. C* **68**, 051001(R) (2003).
- [44] K. Ermisch, H. R. Amir-Ahmadi, A. M. van den Berg, R. Castelijns, B. Davids, A. Deltuva, E. Epelbaum, W. Glöckle, J. Golak, M. N. Harakeh, M. Hunyadi, M. A. de Huu, N. Kalantar-Nayestanaki, H. Kamada, M. Kiš, M. Mahjour-Shafiei, A. Nogga, P. U. Sauer, R. Skibiński, H. Witała, and H. J. Wörtche, *Phys. Rev. C* **71**, 064004 (2005).
- [45] W. P. Abfalterer, F. B. Bateman, F. S. Dietrich, R. W. Finlay, R. C. Haight, and G. L. Morgan, *Phys. Rev. C* **63**, 044608 (2001).
- [46] K. Schoen, D. L. Jacobson, M. Arif, P. R. Huffman, T. C. Black, W. M. Snow, S. K. Lamoreaux, H. Kaiser, and S. A. Werner, *Phys. Rev. C* **67**, 044005 (2003).
- [47] A. Deltuva, A. C. Fonseca, and P. U. Sauer, *Phys. Rev. C* **72**, 054004 (2005).
- [48] A. Deltuva (private communication, 2018).
- [49] H. Witała *et al.*, *Few Body Syst.* **57**, 1213 (2016).
- [50] A. C. Phillips, *Nucl. Phys. A* **107**, 209 (1968).
- [51] H. Witała, A. Nogga, H. Kamada, W. Glöckle, J. Golak, and R. Skibiński, *Phys. Rev. C* **68**, 034002 (2003).
- [52] B. D. Carlsson, A. Ekström, C. Forssén, D. F. Stromberg, G. R. Jansen, O. Lilja, M. Lindby, B. A. Mattsson, and K. A. Wendt, *Phys. Rev. X* **6**, 011019 (2016).



- [53] H. Witała, T. Cornelius, and W. Glöckle, *Few-Body Syst.* **3**, 123 (1988).
- [54] D. Hüber *et al.*, *Acta Phys. Pol. B* **28**, 1677 (1997).
- [55] W. Glöckle, *The Quantum Mechanical Few-Body Problem* (Springer-Verlag, Berlin, 1983).
- [56] W. Tornow, R. C. Byrd, C. R. Howell, R. S. Pedroni, and R. L. Walter, *Phys. Rev. C* **27**, 2439 (1983).
- [57] S. A. Coon and H. K. Han, *Few-Body Syst.* **30**, 131 (2001).
- [58] B. S. Pudliner, V. R. Pandharipande, J. Carlson, S. C. Pieper, and R. B. Wiringa, *Phys. Rev. C* **56**, 1720 (1997).
- [59] W. Tornow and H. Witała, *Nucl. Phys. A* **637**, 280 (1998).
- [60] H. Witała, J. Golak, R. Skibiński, and K. Topolnicki, *J. Phys. G* **41**, 094011 (2014).
- [61] J. Golak *et al.*, *Eur. Phys. J. A* **50**, 177 (2014).
- [62] A. Margaryan, R. P. Springer, and J. Vanasse, *Phys. Rev. C* **93**, 054001 (2016).
- [63] H. Witała, W. Glöckle, J. Golak, A. Nogga, H. Kamada, R. Skibiński, and J. Kuroś-Zołnierczuk, *Phys. Rev. C* **63**, 024007 (2001) and references therein.
- [64] K. Hatanaka, Y. Shimizu, D. Hirooka, J. Kamiya, Y. Kitamura, Y. Maeda, T. Noro, E. Obayashi, K. Sagara, T. Saito, H. Sakai, Y. Sakemi, K. Sekiguchi, A. Tamii, T. Wakasa, T. Yagita, K. Yako, H. P. Yoshida, V. P. Ladygin, H. Kamada, W. Glöckle, J. Golak, A. Nogga, and H. Witała, *Phys. Rev. C* **66**, 044002 (2002).
- [65] Y. Maeda, T. Kawabata, K. Suda, H. Sakai, K. Fujita, K. Hatanaka, H. Okamura, Y. Sakemi, Y. Shimizu, Y. Tameshige, A. Tamii, M. B. Greenfield, M. Hatano, H. Kuboki, T. Saito, M. Sasano, K. Yako, J. Kamiya, J. Rapaport, K. Sekiguchi, T. Wakasa, J. Blomgren, P. Mermod, A. Ohn, M. Osterlund, H. Witała, J. Golak, R. R. Skibiński, A. Deltuva, A. C. Fonseca, P. U. Sauer, W. Glöckle, H. Kamada, and A. Nogga, *Phys. Rev. C* **76**, 014004 (2007).
- [66] H. Shimizu *et al.*, *Nucl. Phys. A* **382**, 242 (1982).
- [67] B. R. Barrett, P. Navrátil, and J. P. Vary, *Prog. Part. Nucl. Phys.* **69**, 131 (2013).
- [68] P. Maris, J. P. Vary, and A. M. Shirokov, *Phys. Rev. C* **79**, 014308 (2009).
- [69] P. Maris and J. P. Vary, *Int. J. Mod. Phys. E* **22**, 1330016 (2013).
- [70] S. A. Coon, M. I. Avetian, M. K. G. Kruse, U. van Kolck, P. Maris, and J. P. Vary, *Phys. Rev. C* **86**, 054002 (2012).
- [71] R. J. Furnstahl, G. Hagen, and T. Papenbrock, *Phys. Rev. C* **86**, 031301 (2012).
- [72] S. N. More, A. Ekström, R. J. Furnstahl, G. Hagen, and T. Papenbrock, *Phys. Rev. C* **87**, 044326 (2013).
- [73] K. A. Wendt, C. Forssén, T. Papenbrock, and D. Sääf, *Phys. Rev. C* **91**, 061301 (2015).
- [74] P. Maris, M. Sosonkina, J. P. Vary, E. Ng, and C. Yang, *Proc. Comput. Sci.* **1**, 97 (2010).
- [75] H. M. Aktulga, C. Yang, E. G. Ng, P. Maris, and J. P. Vary, *Concurrency Comput.: Pract. Exper.* **26**, 2631 (2014).
- [76] M. Shao, H. M. Aktulga, C. Yang, E. G. Ng, P. Maris, and J. P. Vary, *Comput. Phys. Commun.* **222**, 1 (2018).
- [77] S. D. Glazek and K. G. Wilson, *Phys. Rev. D* **48**, 5863 (1993).
- [78] F. Wegner, *Ann. Phys.* **506**, 77 (1994).
- [79] S. K. Bogner, R. J. Furnstahl, P. Maris, R. J. Perry, A. Schwenk, and J. P. Vary, *Nucl. Phys. A* **801**, 21 (2008).
- [80] S. K. Bogner, R. J. Furnstahl, and A. Schwenk, *Prog. Part. Nucl. Phys.* **65**, 94 (2010).
- [81] E. D. Jurgenson, P. Navrátil, and R. J. Furnstahl, *Phys. Rev. Lett.* **103**, 082501 (2009).
- [82] R. Roth, J. Langhammer, A. Calci, S. Binder, and P. Navrátil, *Phys. Rev. Lett.* **107**, 072501 (2011).
- [83] E. D. Jurgenson, P. Maris, R. J. Furnstahl, P. Navrátil, W. E. Ormand, and J. P. Vary, *Phys. Rev. C* **87**, 054312 (2013).
- [84] R. Roth, A. Calci, J. Langhammer, and S. Binder, *Phys. Rev. C* **90**, 024325 (2014).
- [85] T. A. Lähde, E. Epelbaum, H. Krebs, D. Lee, Ulf-G. Meißner, and G. Rupak, *Phys. Lett. B* **732**, 110 (2014).
- [86] A. Gezerlis, I. Tews, E. Epelbaum, S. Gandolfi, K. Hebeler, A. Nogga, and A. Schwenk, *Phys. Rev. Lett.* **111**, 032501 (2013).
- [87] A. Gezerlis, I. Tews, E. Epelbaum, M. Freunek, S. Gandolfi, K. Hebeler, A. Nogga, and A. Schwenk, *Phys. Rev. C* **90**, 054323 (2014).
- [88] D. Lonardonì, J. Carlson, S. Gandolfi, J. E. Lynn, K. E. Schmidt, A. Schwenk, and X. B. Wang, *Phys. Rev. Lett.* **120**, 122502 (2018).
- [89] D. Lonardonì, S. Gandolfi, J. E. Lynn, C. Petrie, J. Carlson, K. E. Schmidt, and A. Schwenk, *Phys. Rev. C* **97**, 044318 (2018).
- [90] Z.-T. Lu, P. Mueller, G. W. F. Drake, W. Noertershaeuser, S. C. Pieper, and Z.-C. Yan, *Rev. Mod. Phys.* **85**, 1383 (2013).
- [91] I. Tanihata, H. Savajols, and R. Kanungo, *Prog. Part. Nucl. Phys.* **68**, 215 (2013).
- [92] P. Maris, J. P. Vary, A. Calci, J. Langhammer, S. Binder, and R. Roth, *Phys. Rev. C* **90**, 014314 (2014).
- [93] A. Calci and R. Roth, *Phys. Rev. C* **94**, 014322 (2016).
- [94] E. Caurier, P. Navrátil, W. E. Ormand, and J. P. Vary, *Phys. Rev. C* **66**, 024314 (2002).
- [95] E. Epelbaum, *Phys. Lett. B* **639**, 456 (2006).
- [96] E. Epelbaum, *Eur. Phys. J. A* **34**, 197 (2007).
- [97] S. Ishikawa and M. R. Robilotta, *Phys. Rev. C* **76**, 014006 (2007).
- [98] V. Bernard, E. Epelbaum, H. Krebs, and Ulf-G. Meißner, *Phys. Rev. C* **84**, 054001 (2011).
- [99] L. Girlanda, A. Kievsky, and M. Viviani, *Phys. Rev. C* **84**, 014001 (2011).
- [100] H. Krebs, A. Gasparyan, and E. Epelbaum, *Phys. Rev. C* **85**, 054006 (2012).
- [101] H. Krebs, A. Gasparyan, and E. Epelbaum, *Phys. Rev. C* **87**, 054007 (2013).
- [102] E. Epelbaum, A. M. Gasparyan, H. Krebs, and C. Schat, *Eur. Phys. J. A* **51**, 26 (2015).
- [103] K. Hebeler, H. Krebs, E. Epelbaum, J. Golak, and R. Skibiński, *Phys. Rev. C* **91**, 044001 (2015).